PMMA stability under hydrothermal conditions

Ana Fernández [a], Aránzazu Redondo [a], Judith Martín-de-León [a,b], Danilo Cantero [a,*]

[a] *The Institute of Bioeconomy. Calle Dr Mergelina S/N, Department of Chemical Engineering and Environmental Technology, University of Valladolid, Valladolid 47011, Spain*
[b] *Cellular Materials Laboratory (CellMat), Condensed Matter Physics Department, University of Valladolid, Valladolid 47011, Spain*

HIGHLIGHTS

- PMMA is highly stable at hydrothermal conditions, up to 200 °C and 6 h of treatment.
- The temperature cycle promotes the trapping of water droplets in the polymer.
- Plasticize effect of water molecules plays an important role in Tg of the polymer.

GRAPHICAL ABSTRACT
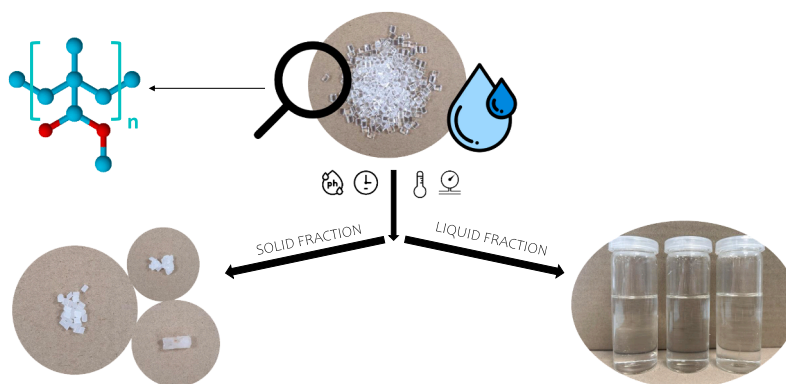
ARTICLE INFO

ABSTRACT

PMMA is a synthetic polymer of methyl methacrylate. PMMA is used widely in many applications and the interest in their physicochemical properties is growing. In this work, a hydrothermal study was carried out to evaluate the PMMA stability under hydrothermal conditions (up to 200°C), pH (2−10) and reaction time (up to 360 min). The water-PMMA system is affected by different mechanisms when dosed with bases or acids suggesting predominantly an interaction of ester groups with the medium. The results prove that the polymer is highly stable at the tested conditions. It is observed that water molecules are encapsulated in the polymer due to the softening and hardening during the process. This phenomenon was seen in the thermogravimetric analysis. The glass transition temperature of PMMA was slightly reduced after the treatment. This suggests that the hydrothermal process promotes the degradation of the shortest polymeric chains.

1. Introduction

Poly(methyl methacrylate) (PMMA, -[C$_5$O$_2$H$_8$]$_n$-) belongs to the class of thermoplastic polymers. It is a synthetic polymer of methyl methacrylate (MMA). PMMA can be made not only by free radical polymerization, ionic polymerization and coordination polymerization of MMA; but also, by the esterification of PMAA (poly(methacrylic acid)) [1]. The first solid PMMA sheet was developed by the German firm,

Rohm & Haas AG in the mid-1920 s. However, it was not commercialized until 1931 by Rowland Hill of Imperial Chemical Industries (ICI's) Dyestuffs Division (North England) [2]. PMMA belongs to the acrylic polymer family and is known by trademarks such as Lucite, Perspex, Oroglas, Goldglas, Altuglas. The production of PMMA is estimated as 3.9 million metric tons per year and it had a demand increased by 25% in 2020 [3,4].

Compared to ordinary glass, PMMA is more transparent, twice lighter and up to eight times less brittle. It is easy to mold into a variety of shapes and shows high mechanical strength, high transmittance, surface hardness, abrasion resistance, thermal and chemical stability, and excellent weatherability [5,6]. PMMA and PMMA-based materials are used in multiple fields and applications, such as biomedicine, molecular separation, optical science, electrical insulation, composing in polymer electrolytes, viscosity applications, pneumatic actuation, sensing technology, nanotechnology and solar applications due to their versatile properties [6].

The environmental problems caused by using fossil fuels as an energy source, combined with the depletion of these resources, have led to a growing interest in alternative energy sources. In recent years, there was an urgent demand for alternatives to promote the sustainable development of different materials. In this context, PMMA plays an important role as a sustainable material and an eco-friendly alternative to standard polymers. It is generally accepted that PMMA is non-toxic as it contains less potentially harmful subunits from the synthesis compared to other polymers. Moreover, the reagents to make the polymer have been recently produced from renewable sources [7]. This effort seeks the full or partial replacement of synthetic materials and contribute to reduced energy consumption and CO_2 emissions. In addition, PMMA can be used for energy efficiency and chemical or mechanical recycling. For example, recycling PMMA to MMA via thermochemical technologies allows this monomer to be reused as a source of PMMA or other acrylic-based polymers [4,8]. Finally, the PMMA is a thermoplastic that allows re-using it many times.

Our research team is currently working on novel processes for making PMMA-based materials. Understanding the stability or changes that the polymer experiences when subjected to hydrothermal conditions has been identified as an important research gap. The physical properties of polymers could be influenced by its internal structure and the temperature and pressure history. The thermal degradation [9–11] and the glass transition temperature [12–14] of PMMA have been studied extensively; however, limited data are available on the PMMA stability in water under different conditions of temperature, time and pH. In this work, the effect of pH, temperature and time on PMMA dispersed in water was evaluated. The starting material and solid products were analyzed by gel permeation chromatography (GPC) for molecular weight distributions and by differential scanning calorimetry (DSC) and thermogravimetric analysis (TGA) analysis to determine the glass transition temperature and thermal stability, respectively. Scanning electron microscope (SEM) analysis was conducted to evaluate changes in the morphology. Total organic carbon (TOC) analysis was carried out to determine the amount of polymer leached to the water phase.

2. Materials and methods

2.1. Material and reagents

PMMA Plexiglas® 7 N of Roehm GmbH in the form of pellets (2.35 mm diameter and 3 mm long) was kindly supplied by PLEXIGLAS® Evonik Industries (Essen, Germany). The number 7 describes an affiliation to a group of PMMA having similar chemical properties and the subsequent letter N stands qualitatively for a low viscosity level of the melt.

Ultrapure water (18.2 MΩ•cm, collected from a Milli-Q® water purification system), sulphuric acid (72%, PanReac®) and sodium
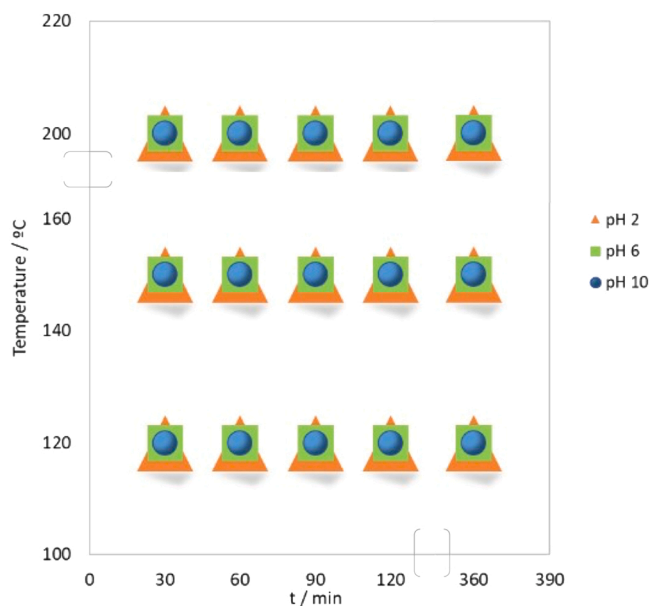

Fig. 1. Experimental design.

hydroxide (98%, PanReac® pellets) were used as the reaction medium to run the experiments. Ultrapure water and tetrahydrofuran (99.9%) were used as the mobile phase in the GPC analysis.

2.2. Methodology

2.2.1. Experimental conditions

The PMMA samples were subjected to hydrothermal reactions to evaluate the changes over different conditions of pH, temperature and time. An experimental design of 45 assays shown in Fig. 1 was developed to study the polymer stability under such conditions. The pH developed by PMMA in water (~20% w/w) was 6. The effect of acidity or basicity was also evaluated by dosing with sulfuric acid (pH=2) or sodium hydroxide (pH=10). Three temperatures were selected to evaluate the thermal stability, 120, 150 and 200°C. The pressure was not controlled during treatment, and the pressure generated inside the reactor was the saturation pressure of water at the experimental temperature. For the highest temperature, 200°C, the reactor pressure was around 15.3 bar. Treatment times tested were 30, 60, 90, 120 and 360 min. The pH values of 4 and 8 were tested at a temperature of 200 °C and reaction time of 360 min for better monitoring the evolution of the final process pH versus the initial pH. Three independent replicated samples from hydrothermal treatments were carried out.

A given amount of polymer (~11,9 g) was mixed with ~40 mL of deionized water (pH=6) and placed in a stainless-steel reactor (25.4 mm outer diameter, 22.2 mm inner diameter, 250 mm long and 70 mL internal volume). The reactor was sealed by Gyrolok® type fittings. A constant acid (~0.11% v/v) or basic (~0.04%w/w) concentration was added to the aqueous solution to evaluate the pH effect. A resulting value of about 2 or 10 was obtained for the acid or basic condition, respectively. The reactor was placed in vertical position to ensure that the solid was completely submerged in the aqueous medium. After the heating treatment in a convection oven (Heratherm, Thermo Scientific, Germany) the reactor was cooled down to room temperature (25 °C) by letting the reactor stand at lab air conditions for 60 min. The mixture was filtered (filter ashless paper, 14–18 μm) to separate the liquid from the insoluble solid. At least three assays, with independent sample collection and preparation, were performed to verify the consistency of the results. For each solution, initial and final pH values were measured using a BASIC 20 pH-meter at 25°C. The labels for the samples were created by using the following code: Temperature (°C) – pH – time
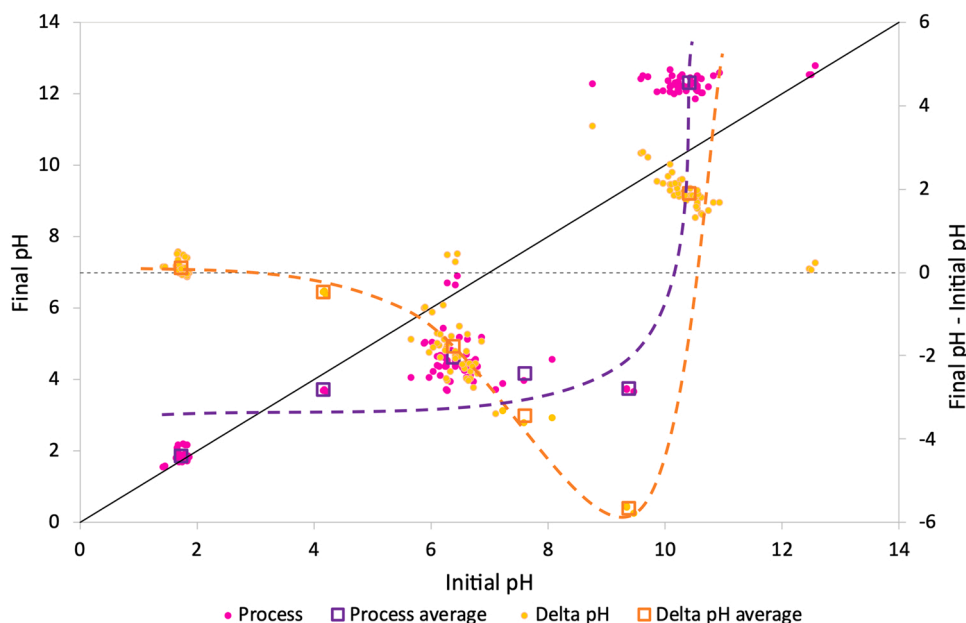
Fig. 2. Evolution of the pH in the reactor. The solid black line shows a diagonal and the dotted black one represents a horizontal line at zero delta pH. Pink dots represent the pH after the treatment. Yellow dots show the difference between the final and initial pH. Treatment times tested were 30, 60, 90, 120 and 360 min.(For interpretation of the references to color in this figure legend, the reader is referred to the web version of this article.)

(min).

2.2.2. Analytical techniques

2.2.2.1. Total organic carbon.
The total organic carbon (TOC) contained in the liquid fraction was determined with a TOC analyzer (Shimadzu TOC-VCSH, Japan). This measurement was used to evaluate the amount of polymer degraded or leached to the water after the hydrothermal treatment.

2.2.2.2. Gel permeation chromatography.
The molecular weight of the solid samples was determined by gel permeation chromatography (GPC) in the "Centro de Investigación en Tecnoloxías Navais e Industriais (Citeni)" at the Universidade da Coruña in Ferrol (Spain). GPC was used to obtain number-averaged molecular weights (Mn), weight-averaged molecular weights (Mw), and polydispersity index (Mw/Mn) of the PMMA-derived solids. To carry out this measurement, all samples (except the original PMMA) were dried in a vacuum oven at 50°C for 24 h. The samples were first dissolved in tetrahydrofuran (THF) to a concentration of 1300 mg/L and filtered through a 0.2 μm polyamide filter. The results reported are an average of three replicates for each sample.

The GPC analyses were carried out using a Waters HPLC Alliance 2695 separations module (Waters, Mildford, MA, USA) with a set of three Styragel Waters columns connected in series (HR 5E, HR 4E, HR 3; 300 mm length x 4.6 mm internal diameter, packed with 5 μm nominal particle size) covering a molecular weight range of 2,000- 4000,000, 50–100,000 and 500–30,000; respectively. A Styragel guard column was installed to trap any particles that may potentially plug the columns. THF was used as an eluent at a flow rate of 0.3 mL/min. Measurements were performed at 35°C using a refractive index (RI) detector (Waters, model 2410). The injection volume was set at 10 μl. Molecular weights of polymers were referenced to polystyrene standards provided by the Polymer Standards Service GmbH (Mainz, Germany). Data was collected using Empower 2 software Waters Corporation (Waters, Mildford, MA, USA).

2.2.2.3. Scanning electron microscopy.
An environmental scanning electron microscopy (FEI QUANTA 200 FEG ESEM, FEI Company Czech Republic) was used to study the surface characteristics and elemental composition of the samples. The liquid samples were analyzed under low-vacuum conditions, whereas the solids samples were characterized using a secondary electron detector (an Everhart–Thornley detector (ETD) and a large-field detector (LFD), respectively). Micrographs were obtained at 500 × and 3000x magnification. Energy Dispersive Spectroscopy (EDS) data was collected with an EDAX Genesis module coupled to the ESEM. Solid samples were fractured under liquid nitrogen to obtain images of the cross-section.
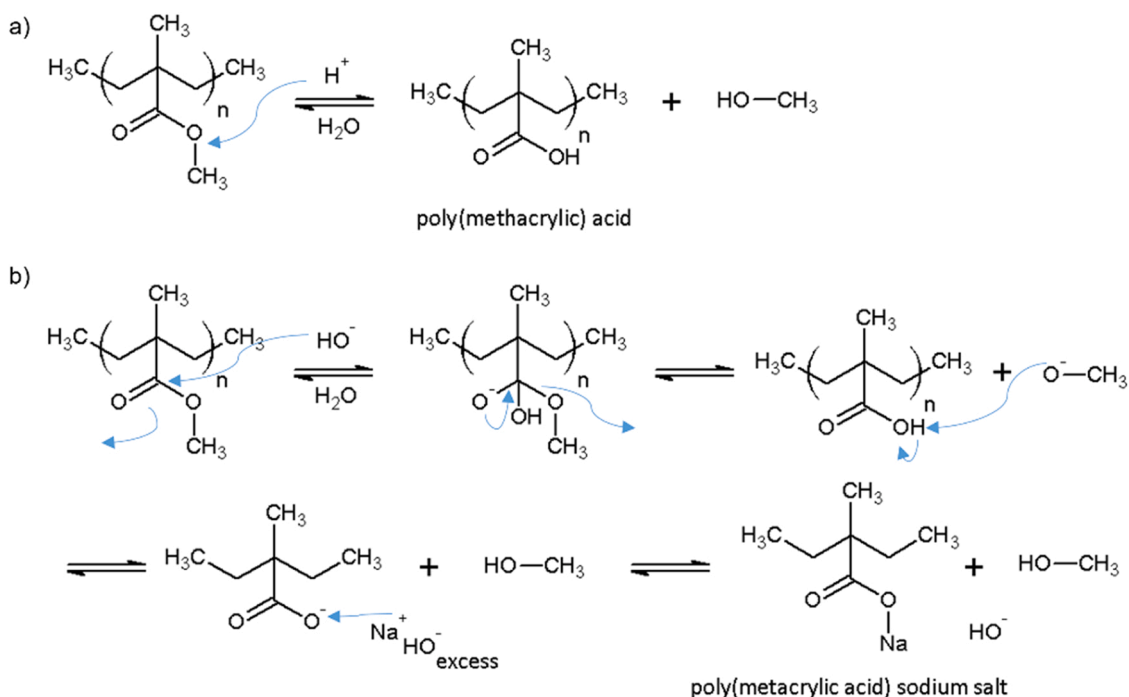
2.3. Thermal characterization

2.3.1. Thermogravimetric analysis (TGA)
Thermal stability was analyzed by TGA in a TGA/SDTA 861 analyzer of Mettler Toledo (Mettler-Toledo S.A.E., L'Hospitalet de Llobregat, Barcelona, Spain). The experiments were carried out using 15 mg of the sample in a nitrogen atmosphere with a flow rate of 60 mL/min at the heating rate of 20°C/min from room temperature (25 °C) to 650°C. At 650°C, the purge gas flowing over the sample was automatically switched to oxygen and the carbon residue was burned off at 850°C. The heating and flow rates employed were the same as the previous stage. The heating rate was selected to be high enough to minimize time analysis and avoid any overlapping. The derivative of the weight loss curve (DTG curve) was calculated, and the temperature of maximum volatile matter evolution (T_{max}) was derived from the TG/DTG curves.

2.4. Differential scanning calorimetry (DSC)

Additional thermal analysis was performed on the solid products to determine their glass transition temperature (Tg) using a Differential Scanning Calorimeter DSC 3 + from Mettler Toledo (Mettler-Toledo S.A. E., L'Hospitalet de Llobregat, Barcelona, Spain). Samples with a mass of approximately 10–15 mg were heated to 160 °C at a rate of 10 °C/min, and subsequently cooled to 30 °C at the same rate in the cooling cycle. The aim was to remove any processing history to the polymer. The same heating steps were repeated for a second scan. A flow of 60 mL/min of N_2 was used to ensure an inert atmosphere and consequently hinder the mass gains associated with the oxidation. A low heating rate was

Scheme 1. Schematic representation of PMMA mechanisms under a) acid and b) alkaline pH aqueous media.

selected to avoid uncertainties in Tg measurement.

The thermal characterization was evaluated using the STAR^e software version 16.00 (Mettler-Toledo S.A.E., L'Hospitalet de Llobregat, Barcelona, Spain). The glass transition temperature was determined at the inflection point between the onset and the end-set temperatures.

### 2.4.1. Inductively coupled plasma mass spectrometry

The liquid products were subjected to heavy metals analysis by ICP Mass Spectrometry (ICP-MS with Agilent HP 7500c Octopolar Reaction System, Agilent Technologies International Japan, Ltd., Yokyo, Japan). These results were relevant to evaluate the reactor (stainless steel) stability under hydrothermal, acidic, and basic conditions.

3. Results and discussion

The results were analyzed in two groups: the liquid product (Section 3.1) and the solid product (Section 3.2).

3.1. Liquid product characterization

The liquid product was analyzed by measuring the pH of the medium, the amount of carbon in the liquid and the metals composition.
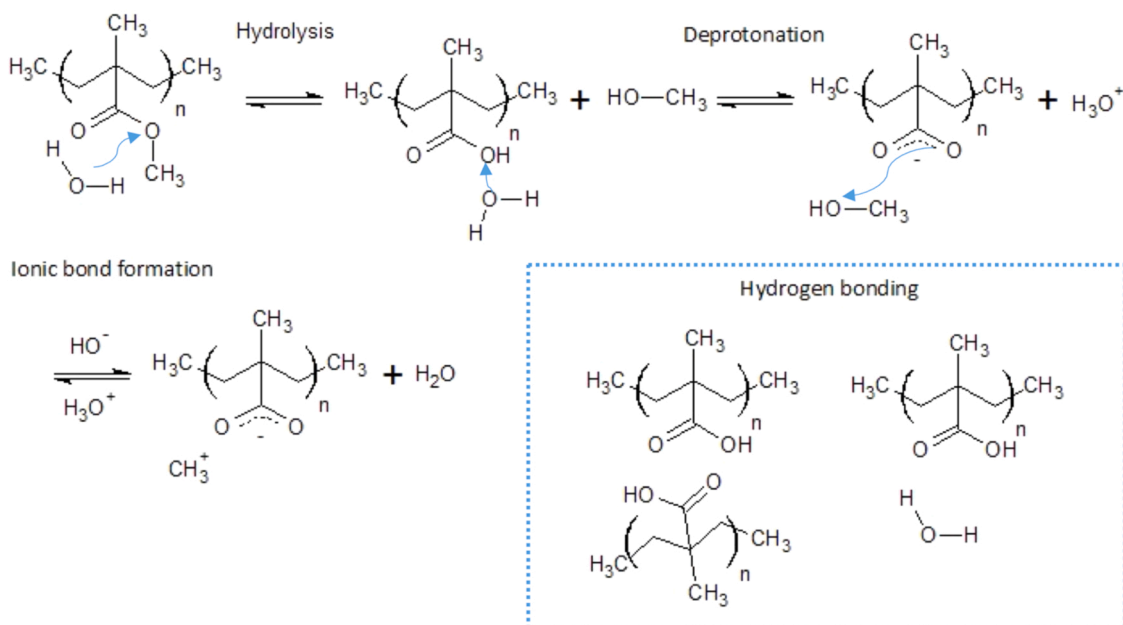
Scheme 2. Schematic representation of PMMA mechanism under neutral media. Effect of the water on the formed bonds.
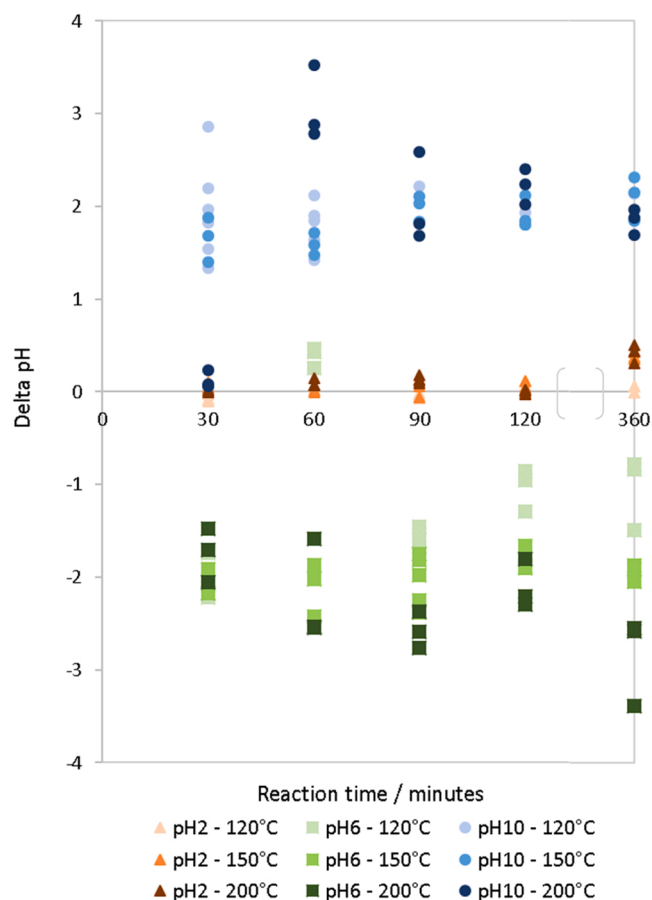
Fig. 3. Evolution of the pH difference (delta pH) over the time at the experimental temperature conditions. The blue dots represent base-hydrothermal conditions. The red dots represent acid-hydrothermal conditions, and the green dots show the unmodified-hydrothermal conditions. The temperature is represented by the shade of the color. The lighter, the cooler and the darker, the hotter. (For interpretation of the references to color in this figure legend, the reader is referred to the web version of this article.)

3.2. The influence of pH

The pH was measured before and after the hydrothermal treatment. It was observed that the pH was noticeably modified after the treatment for the clusters of experiments for alkaline and unmodified pH conditions. The pH of the final product slightly changed (less than 0.1) for the acidic conditions (pH=2).

Fig. 2 shows the evolution of the pH for all the experiments. The pink dots show the pH after the treatment. Three different behaviors can be seen. The pH remains almost unchanged when the initial pH was around 2. For these acidic conditions, the pH is similar to the initial pH or slightly higher (less than half pH unit). More clear effects were seen for the unmodified or basic conditions. An increase of ~3.5 units in alkaline medium occurs after reaction, whereas the pH of the unmodified medium is reduced by ~3.4 units. The dashed golden line in Fig. 2 shows the pH change after the process depending on the initial pH. This line does not represent any modelling, its goal is to facilitate the data analysis. The pH change is negative (creates a more acid medium) when operating at initial pH between > 2 and < 9. Below 2 the pH is slightly modified. Above 10, the pH is increased after the treatment (creates a more basic medium).

Two levels of pH were added (pH=4 and 8) to monitor the evolution of the pH and two dotted curves lines were drawn to show a tendency. It seems that as the initial pH increases, the final pH remains almost constant until it reaches the value of ≈ 9.7. From this pH value, the final

pH increases considerably (purple dotted curve). The yellow dotted curve shows a pronounced change in delta pH, describing an inflection point at pH≈ 9.7.

Different mechanisms can explain the pH behavior when the hydrothermal treatment is carried out under basic, acid, or neutral stimulus. The Scheme 1 shows potential acid/base behavior for the polymer under these conditions. It can be speculated that the methoxy group of the MMA is attacked by a proton under acidic and unmodified media. On the other hand, the carbonyl group is attacked under alkaline media.

1. The treatment under acidic conditions leads to the formation of PMAA units and methanol. The acid reacts with the sterically accessible pendant methoxy group, which is transformed into an alcohol. The pH of PMAA in water is ~3.1, then the decrease in pH is expected for unmodified pH conditions. The release of PMAA to the medium when running acidic conditions (Initial pH ~2) slightly increases the pH because PMMA is less strong than sulfuric acid.
2. The alkaline medium differs in that the nucleophilic hydroxide attacks the electrophilic carbon of carbonyl group, since hydroxide is more reactive than water. Under alkaline conditions a free alcohol is formed, while the remaining part of the side chain will end with a carboxyl group, which may be protonated afterward to form PMAA [15,16]. However, due to the observed pH increase, free Na^+ ions (due to an excess of NaOH) could protonate the carboxylic group to produce units of the corresponding salt.
3. In the case of unmodified medium, the polymer is only exposed to a neutral water solution that may cause hydrolysis. This reaction will affect the ester group, according to the scheme shown in Scheme 2. As a result, the methyl methacrylic units are converted into of methacrylic acid (without backbone chain scission). Subsequently, hydrogen bonds could be formed between the hydroxyl and the carbonyl groups of adjacent PMMA chains and/or by the water molecules at the interface [17–19].

Fig. 3 shows the evolution of the pH with reaction time for different temperatures and initial pH. The change in the pH is higher as the temperature increases, however, there is not a confirmed trend between these two variables. Although some differences could be evaluated in the behavior of pH at different temperatures and reaction time, they do not show a clear trend. It can be mentioned though, that the pH is mainly change in the first 30 min of reaction and then the changes are less pronounced.

3.3. Carbon balance

A carbon mass balance was conducted to identify the fraction of PMMA that is found in the liquid products. This balance was calculated as shown in Eq. 1, where C_l is the percentage of initial PMMA carbon found in the liquid product; C_{TOC} is the carbon in the liquid product measured by TOC and C_{PMMA} is the amount of carbon loaded to the reactor as polymer.

$$C_l(\%) = \frac{C_{TOC}}{C_{PMMA}} 100\% \qquad (1)$$

Fig. 4 shows the evolution of the carbon leached that PMMA undergoes under the specific hydrothermal conditions of temperature (120, 150, 200°C), pH (2, 6, 10), and time (30, 60, 90, 120, 360 min). The fraction of carbon leached is rather low for unmodified and acid media, covering all the temperature and time ranges (below 0.2% w/w). A substantial increase (still low in absolute numbers) is observed under alkaline medium. When a pH= 10 is applied, carbon leached reaches the value of 0.15% w/w at 150°C and t = 360 min; becoming relevant at the highest temperature and longer reaction times (T = 200°C, pH=10, t = 360 min; ~0.6% w/w). In any case the amount of polymer found in the liquid fraction was always low, below 0.6% w/w. This suggests that the polymer is stable under these conditions.
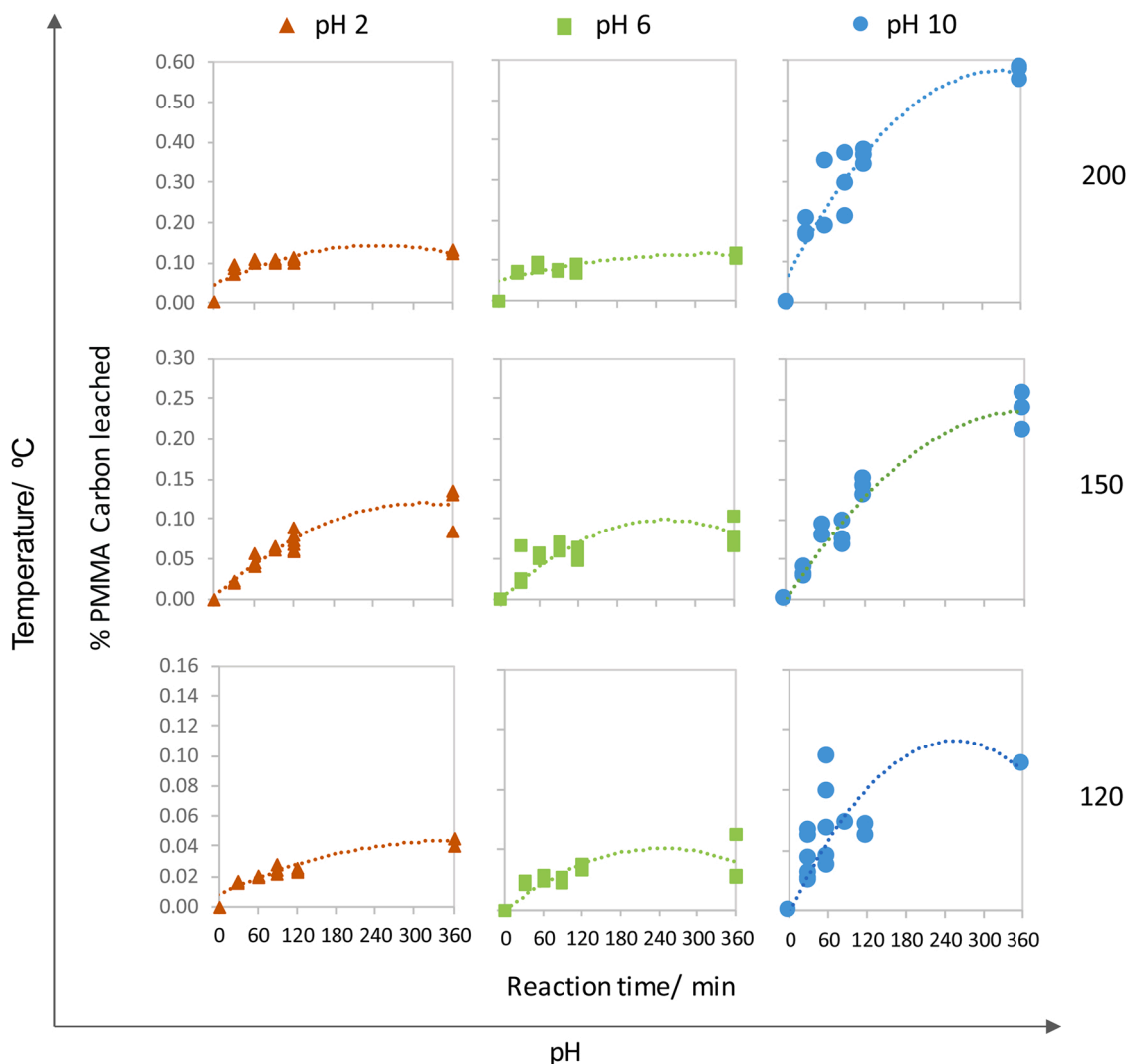
Fig. 4. Carbon balance of the different assays. The lines do not represent any kinetic modelling, it is included to guide the eye to follow the trend.

Table 1
PMMA-derived solids obtained after hydrothermal treatment.

Sample (T-pH)[d]	Mn[a] (g/mol) Mean ± SD	Mw[b] (g/mol) Mean ± SD	PDI[c] Mean ± SD
PMMA	43,600 ± 1200	79,100 ± 2200	1.82 ± 0.03
120–2	43,400 ± 1900	79,200 ± 2300	1.82 ± 0.05
200–2	44,000 ± 700	80,600 ± 1200	1.80 ± 0.05
120–6	45,500 ± 600	81,100 ± 1800	1.81 ± 0.03
200–6	44,800 ± 1600	81,000 ± 2000	1.81 ± 0.04
120–10	44,000 ± 1000	80,500 ± 1200	1.83 ± 0.03
200–10	45,400 ± 1900	81,400 ± 2400	1.79 ± 0.03

[a]The number average molecular weight, [b]The weight average molecular weight, [c]Polidispersity index; [d]Solids obtained under the indicated conditions of temperature and pH (T-pH) at the time of 360 min. SD (standard deviation) of the mean for three measurements of independent replicated samples.

3.4. Solid product characterization

3.4.1. Molecular weight determination

Table 1 summarizes the main characteristics measured by GPC. These are: number average molecular weight (M_n), the weight-average molecular weight (M_w) and the polydispersity index (PDI) calculated using Eq. 2. The analyses were done to PMMA before and after the hydrothermal treatment. Due to high number of samples, only few relevant samples were chosen. Those samples were produced at two
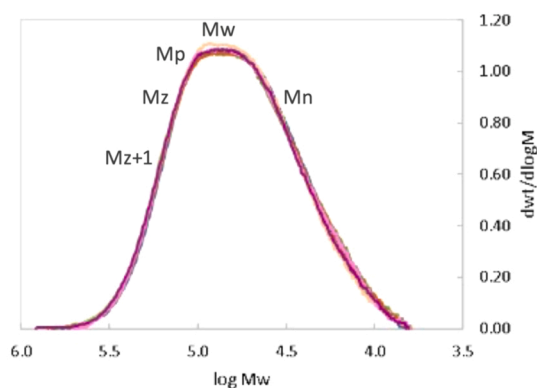

Fig. 5. Molecular weight distribution (MWD; GPC analysis, RI detection) of PMMA before and after being exposed to different conditions. Measured in THF against polystyrene standards (T = 120, 200°C, pH=2,6,10, t = 360 min).

temperatures (120, 200°C), different pH conditions (pH 2, 6, 10) after 6 h of reaction time.

$$PDI(\%) = M_w/M_n \qquad (2)$$

The pristine PMMA shows a molecular weight of 79,142 g/mol with

Table 2
Extracted data from TGA, DTG, and DSC curves for PMMA and PMMA-derived solids.

Sample	TGA		DTG			[d]DTGmax$_3$ (1/°C)	DSC			
	Step 1 + 2	Step 3	Step 1	Step 2	Step 3		1st heating			2nd heating
T (°C)-pH[a]	%Weight loss		Tmax[c] / °C				T / °C			
			Tmax$_1$	Tmax$_2$	Tmax$_3$		[e]Tg $_1$		[f]Tm	[e]Tg$_2$
PMMA[b]	-	99.4	-	-	387	-2.13E-02	106		-	108
120–2	1.5	96.1	-	162	387	-2.05E-02	93.0		146	110
200–2	1.5	92.3	130	147	387	-1.96E-02	96.0		145	113
120–6	1.7	94.7	-	164	387	-2.03E-02	93.0		-	109
200–6	4.2	93.2	-	147	390	-2.02E-02	95.0		135	113
120–10	1.9	96.1	-	158	385	-1.97E-02	93.0		> 143	110
200–10	5.4	93.3	153	168	384	-1.99E-02	91.0		> 137	112
200 [g]	-	99.8	-	-	386	-2.13E-02	107			111

[a]Assays at t = 360 min [b]Untreated PMMA [c]Tmax: temperature of maximum volatile matter evolution, [d]DTGmax: maximum rate of volatile matter evolution [e]Tg: glass transition temperature, [f]Tm: melting peak. [g]Solid treated at 200 °C without water.
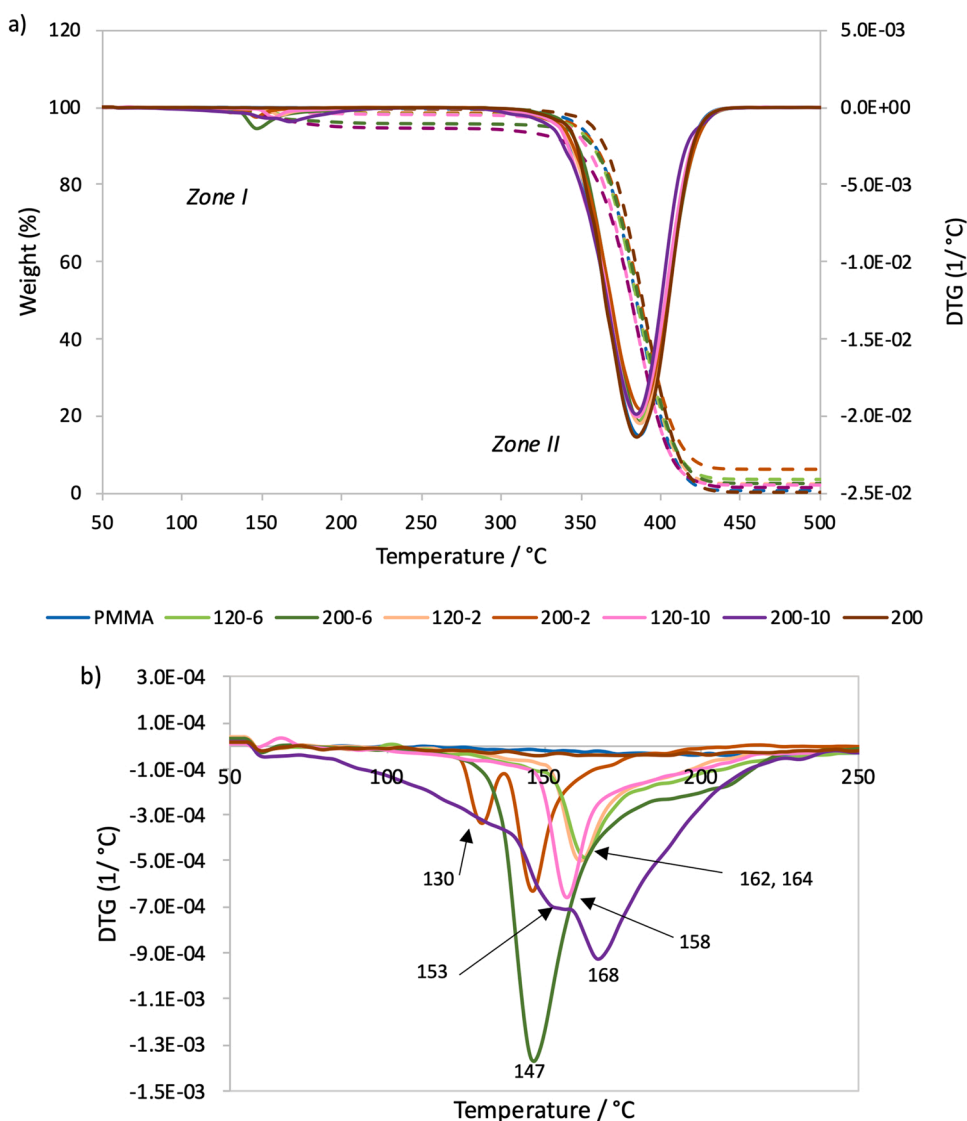

Fig. 6. a) TGA and DTG profiles (dotted lines) of PMMA and the PMMA-derived solids, and b) 50–250°C DTG region. (T = 120, 200°C, pH=2,6,10; t = 360 min; and the solid treat at 200 °C without water).

a polydispersity index of 1.82. A slight increase in the molecular weight (with a maximum of 3% of variation) of all the six treated solids is observed compared to the pristine PMMA. The PDI observed is very similar to those of the same type of PMMA analyzed by other authors [20]. According to this value (PDI average= 1.81), these materials tend to have a high dispersity. This agrees with the broad shape of the molecular weight distribution plot (Fig. 5) [21,22]. A PDI higher than 1 indicates a heterogeneity in the molecular weight distribution, i.e., that
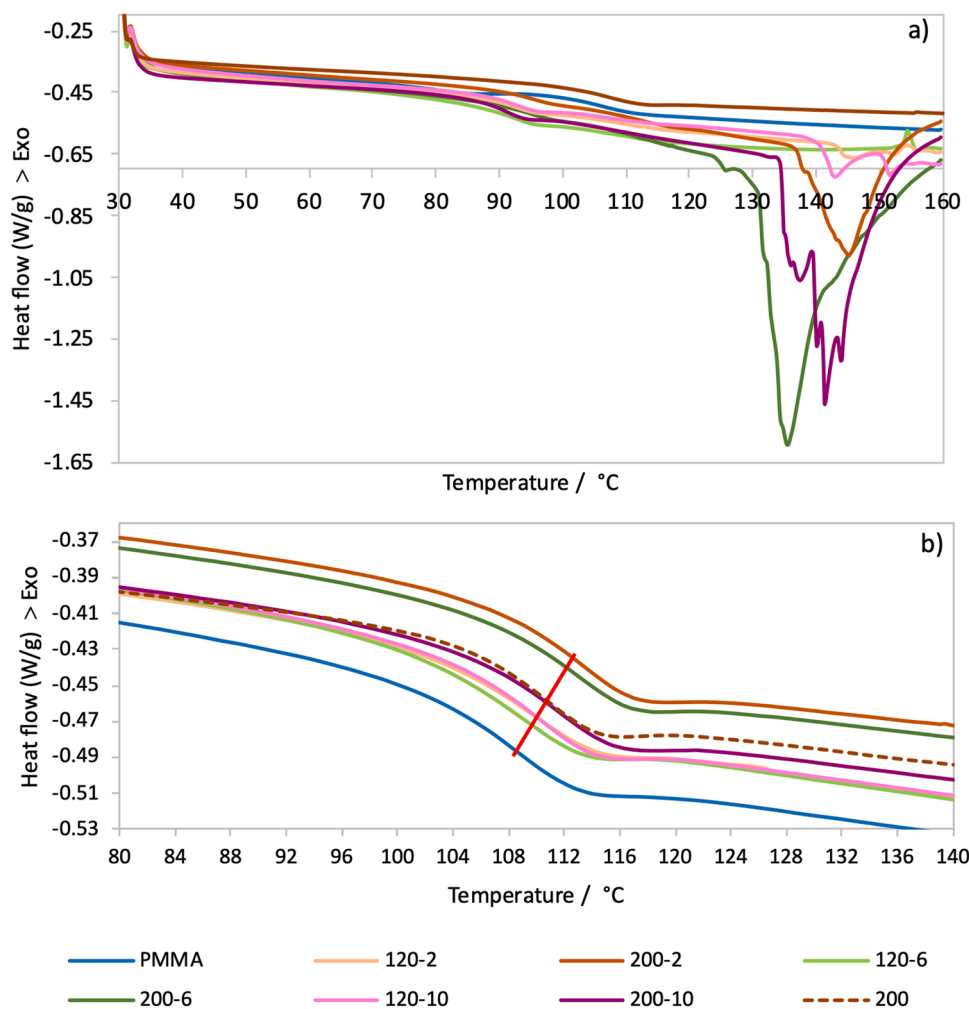
Fig. 7. DSC thermograms for PMMA and the PMMA-derived solids a) at the first heating, and b) at the second heating cycle.

the monomer units are arranged in chains of different length. As for any polydisperse peak, the following trend is fulfilled: $Mn<Mw<Mz<Mz+1$. Only slight changes are observed in the molecular weight of the PMMA-derived solids and the pristine PMMA. A slight increase in the Mw with the treatment temperature could indicate the cleavage of low molecular weight (short chains) giving a lower molecular weight distribution (a lower PDI), but with a higher average molecular weight (Mw) [23]. The thermal behavior is studied and discussed below because the information derived from the study of the molecular weight of the PMMA-solids is insufficient to explain their stability under the applied conditions. However, it cannot be stated that there was a noticeable decomposition during the process and further studies will be required to ensure these criteria.

3.5. Thermal characterization

TGA thermograms of weight loss as a function of temperature (30–650 °C) together with their corresponding differential thermogravimetric (DTG) profiles were studied. Thermal parameters of the PMMA-derived solids are compared to those of the starting PMMA in Table 2. The thermal stability of the untreated PMMA is higher than any of the solid products obtained (see Fig. 6a). The degradation of the PMMA occurs at temperatures above 300°C in one step, suggesting a random scission of the main chains. It was seen in literature that the production process could stabilize the commercial PMMA, and this fact could explain its unique degradation step [24,25]. A single reaction peak is observed in the DTG curve, which confirms that all PMMA products had

decomposed in the form of single reaction. The temperature of maximum volatile matter (Tmax) for untreated PMMA is 387°C (Fig. 6a). An additional assay was carried out (at 200 °C without water) to verify the effect of heating the PMMA without water. The resulting solids had a similar thermal behavior to the starting PMMA. PMMA-derived solids show a different thermal behavior after the hydrothermal treatment. For these solids, two separate steps can be recognized in the TGA/DTG graphs: (i) Zone I (<250°C). PMMA treated solids start to lose weight at around 60°C due to the evaporation of the water molecules. PMMA treated solids treated at 200°C start to degrade earlier and with a slightly higher weight loss than those treated at the lowest temperature (Fig. 6b). These solids could encapsulate more amount of water during the cooling. It should be mentioned that at the highest reaction temperature, an agglomeration occurs, and a white PMMA block is formed. It seems clear that the reaction temperature of the process modifies the polymer structure in a way that could retain water molecules [26]. This statement is confirmed by the higher Mw of the solids treated at 200 °C and will be discussed in section 3.2.3 (Table 2). (ii) Zone II. The most remarkable decomposition zone occurs above 300°C which corresponds to the full decomposition of PMMA, and it is related to the random scission of the polymer chains. The evolution of the maximum temperature for most of the PMMA treated solids at the final stage is similar to that of pristine PMMA (Tmax=387°C, Table 2).

DSC study has been carried out to examine the mobility of PMMA chains in the matrix. DSC thermograms are presented in Fig. 7. In the first heating cycle, glass transition temperature in polymers is not a true second-order transition as it depends on the heating rate (Fig. 7a). The
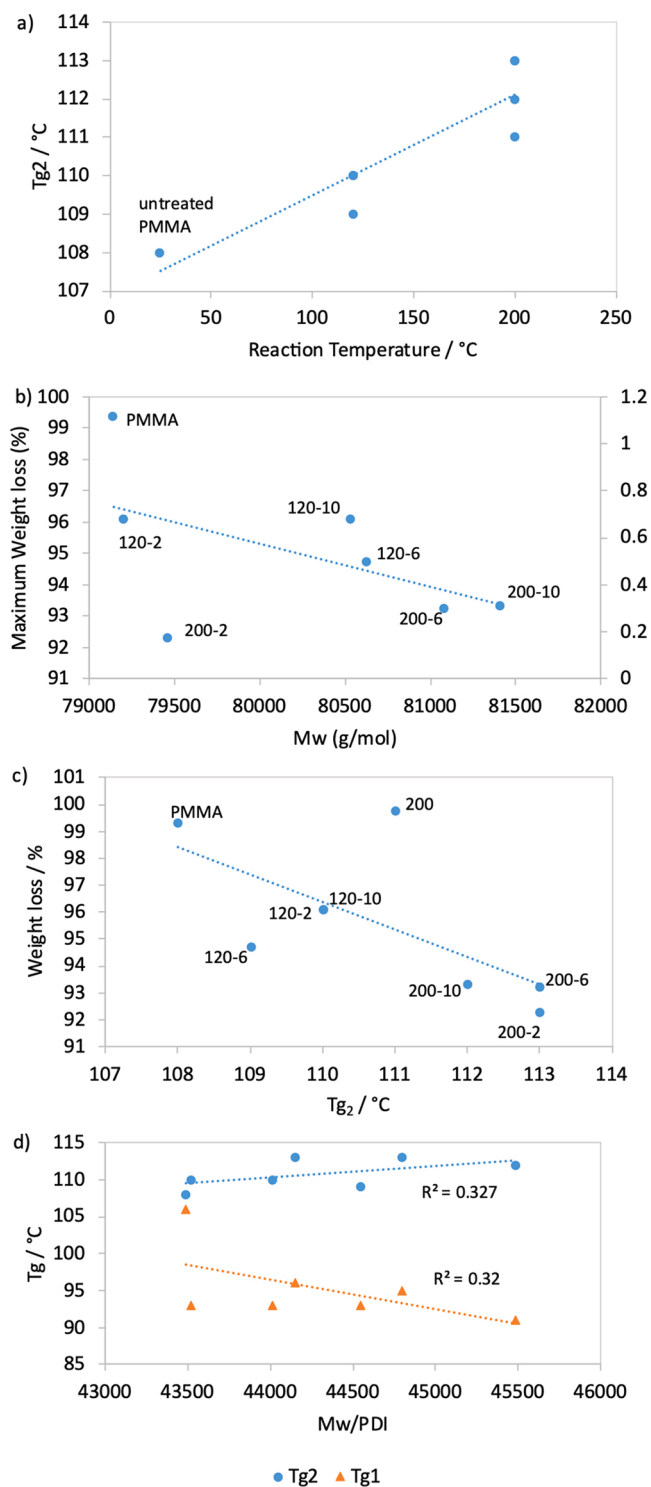
Fig. 8. a) Glass transition temperature (at the second heating cycle, Tg2) against the reaction temperature (25–120–200°C). b) Relationship between weight-average molecular weight and the maximum weight loss for PMMA and PMMA-derived solids (T = 120, 200°C, pH=2,6,10; t = 360 min). c) Tg2 against the maximum weight loss. d) Glass transition temperatures (Tg1, Tg2) against Mw/PDI.

decrease compared to untreated PMMA, (Table 2). Different factors could be responsible for this decrease in Tg_1. It is well known that water molecules act as a plasticizer, which can increase the free volume between polymer chains and increase the chains mobility. This could explain their ability to reduce the glass transition temperature [28,29]. The diminution of Tg_1 could be enhanced because PMMA can absorb 0.3% of water, despite its hydrophobic nature. The maximum drop in Tg_1 between the starting PMMA and PMMA-derived solid is 15°C. This variation in Tg with water content agrees with other authors, that report a 13–19°C of Tg drop [19]. Therefore, a lower Tg could be a reason of less degree of crosslinking and branching, and then, the molecular structure of the solids would be changed [30]. In addition, the hydrothermal treatment temperature plays a role and, as a general trend, the glass transition temperature increases more as the treatment temperate does.

As expected, unprocessed PMMA did not show a fusion peak due to its amorphous nature [31]. The same characteristic is observed for the PMMA solids treated at the lowest temperature without varying the pH (120−6). However, if the temperature is increased and/or the pH is modified (120−2, 120−10, 200−2, 200−6200−10), the corresponding solids show a clear endothermic event, which starts at 135 °C, and it is assigned as the melting transition (crystalline melting endotherm maximum, Tm). Although no crystallization occurs in the PMMA-derived solids (Fig. S1), further studies will be needed to confirm the origin of the endothermic peaks.

It should be noted that significant differences have been observed between the first run and the second one. The second heating cycle only showed a glass transition pattern (Fig. 7b) and Tg_2 of pristine PMMA increases to 108°C. In contrast to the first heating and compared to untreated PMMA, there is a clear trend for Tg_2 to increase with the reaction temperature, as shown in Fig. 8a. It was confirmed that the reaction temperature decreases the weight loss of the PMMA-derived solids, and as shown in Fig. 8, increases their weight-average molecular weight (except for 200−2).

The glass transition temperature evolution at the second heating (Tg_2) as a function of the maximum weight loss is shown in Fig. 8c. The higher Tg_2 correspond to the PMMA treated solids with the lowest weight loss at the highest reaction temperature.

In this work, the low variation in the Mw of the obtained solids does not permit to show a good correlation between Tg and Mw and an opposite trend is observed during the first and second heating, as shown in Fig. 8d The plasticizer effect of the water could be responsible of the decrease of Tg_1, whereas the increase of Tg_2 explains that a depolymerization of shorter chains could take place and the product is composed of longer chains [32].

3.6. Microscopic morphology

As the reaction temperature increases, the transparency begins to disappear and PMMA pellets start to form a homogeneous solid. As commented in the previous section, a white agglomerate can be seen perfectly at 200°C. For this reason, ESEM-EDS was used to examine changes in the surface and cross-section of the PMMA-derived solids. The EDS analysis of solid samples gives an idea about their chemical composition. These samples exhibit peaks that correspond to C and O atoms at the same proportion (the selected area contains an average value of C: 70.08 wt%. and O: 29.92 wt%). This result is consistent with the percentage composition of PMMA (-[$C_5O_2H_8$]n-) per unit of monomer (C: 60%, O: 32%), which indicates that no significant weight loss took place. Moreover, the surface morphology of PMMA and PMMA treated solids shows a rough shape. SEM micrographs show the presence of pores (Fig. 9), and it could be associated to the presence of encapsulated water in their inner structure. No significant changes in the surface structure were seen for the different experimental conditions.
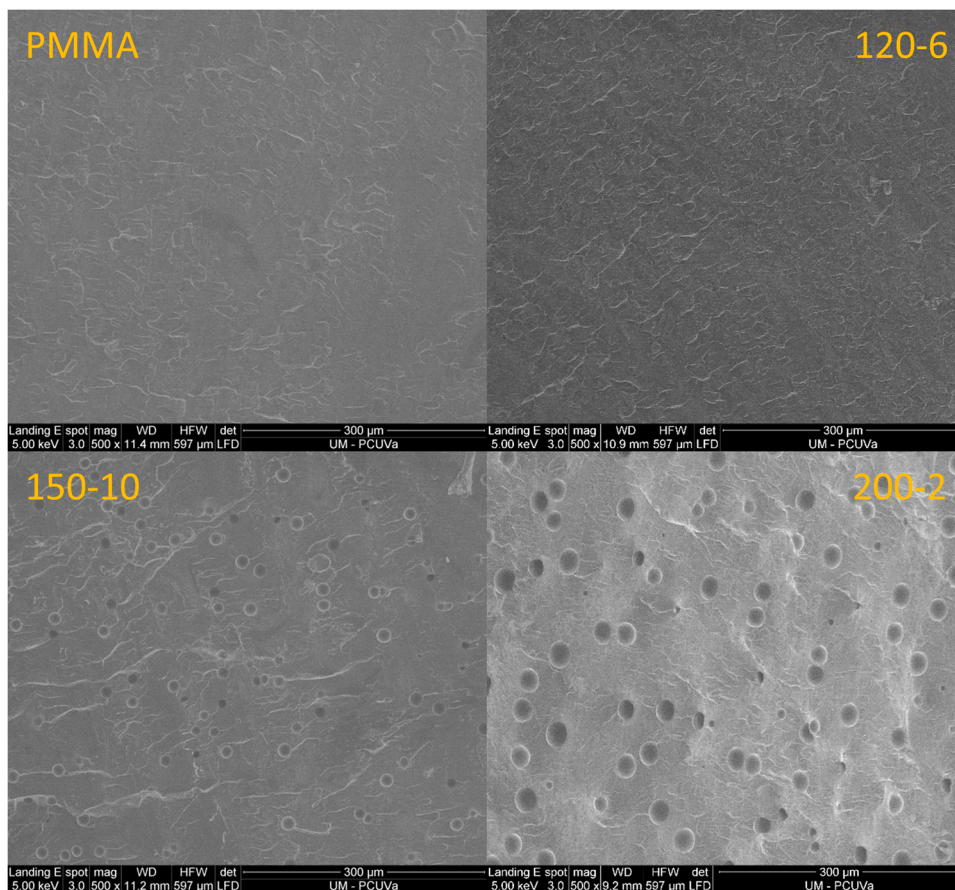
value of 106 °C for PMMA fits with the values reported in the literature [9,12,20]; considering that the Tg_1 of PMMA depends on the degree of tacticity [27]. No first-order transition is observed which indicates the absence of melting temperature and confirms the amorphous character of the matrix polymer. The Tg_1 of PMMA-derived solids showed a

Fig. 9. ESEM analysis of PMMA-derived solids at 5 keV and 500x magnification: a) untreated PMMA b) 120°C-pH= 6, c) 150°C-pH= 10 and d) 200°C-pH= 2 at the processing time of 360 min.
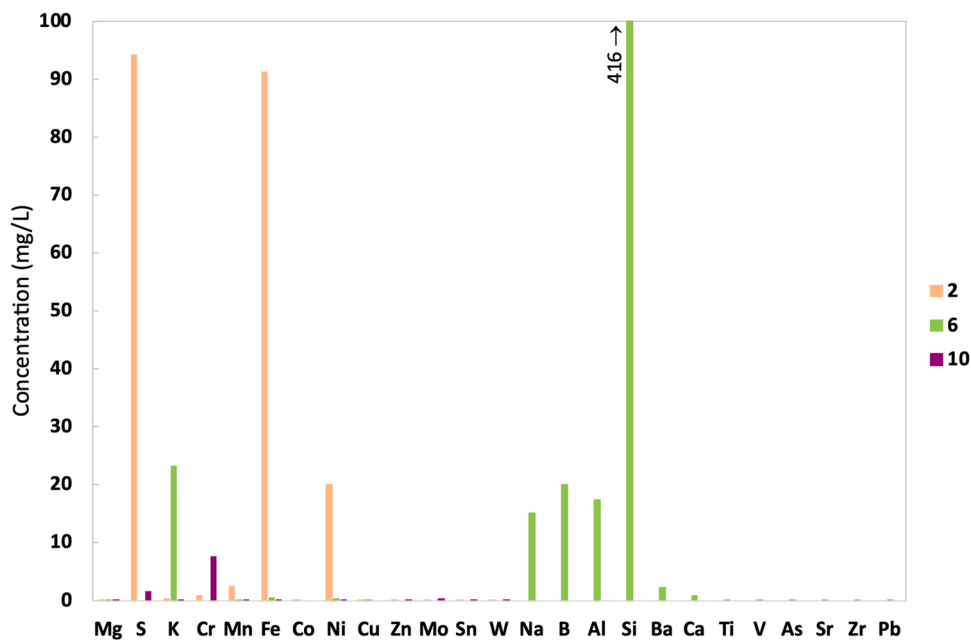

Fig. 10. Elemental composition (mg/L) of liquid products from treatment at different pH levels (pH=2,6,10; T = 200°C, t = 360 min) determined by ICP-MS.

3.7. Reactor and polymer stability

Further studies with the liquid products were carried out to understand if any corrosion took place on the 316 L stainless steel reactor and

the polymer stability. The elemental composition of the type 316 L austenitic stainless steel is characterized by a high concentration of Fe, Cr, Ni and Mo (66% Fe, 18% Cr, 12% Ni, 3% Mo) [33].

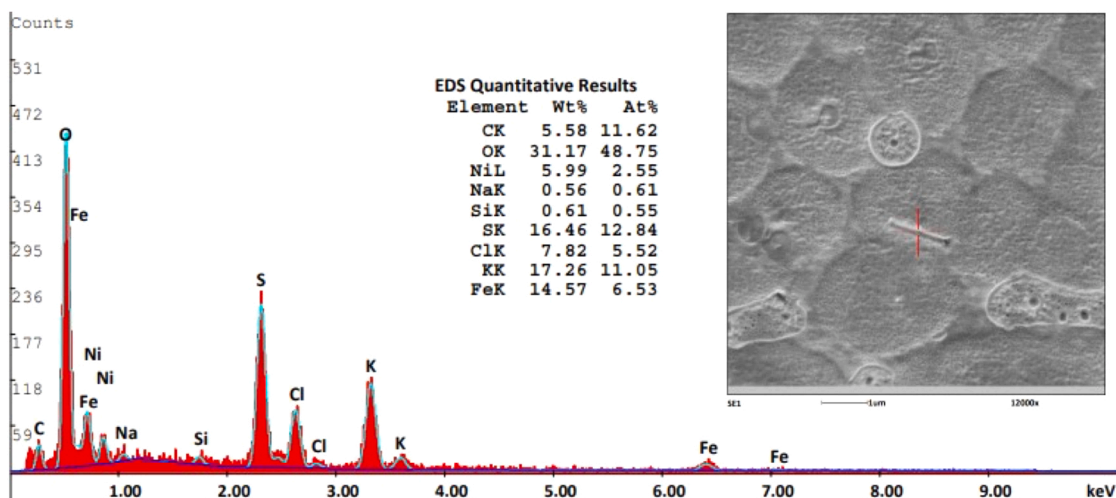An inductively coupled plasma mass spectrometry (ICP-MS) with

Fig. 11. Scanning electron microscopy with energy-dispersive X-ray spectroscopy (ESEM-EDS) analysis of PMMA-derived liquid (200°C-pH=2, 360 min).

semiquantitative analysis was conducted to evaluate the composition of the liquids. The samples chosen were: the 3 levels of pH under the maximum conditions of temperature and time (200°C, 360 min), as shown in Fig. 10. The results indicate significant concentrations of S < Fe << Ni << Mn < Cr in the case of pH= 2; whereas the alkaline liquid is rich in Cr and S. Different composition is found in the neutral liquid (Si << K < B < Al < Na << Ba), which is a remarkable amount of Si. From the data obtained it can be concluded that an acid medium increases the degradation of the 316 L stainless steel due to its high Fe content rather than the alkaline medium. The other elements are in concentrations of less than 2 mg/L.

These results are supported by the SEM analysis. As a further example, Fig. 11 shows an EDS analysis of a PMMA liquid products and they also show similar metals composition. Observations with a scanning electron microscope revealed that particles of Fe and Ni could come from the degradation of the stainless-steel reactor.

4. Conclusions

PMMA offers high stability in water under different conditions of temperature, time, and pH. Hydrolysis was not observed in this experimentation since only slight changes were observed in the weight-average molecular weight. The slight increase in weight-average molecular weight of PMMA treated solids at 200°C suggests a small degradation of the shortest chains of the polymer. The reaction temperature of the hydrothermal treatment and the presence of pores indicates an encapsulation of water molecules. Although the plasticizer effect of water decreases the glass transition temperature, the increase in the glass transition temperature at the second heating cycle suggests that longer chains are formed.

The unmodified medium is the best option to prevent PMMA degradation and low values of carbon material in the aqueous medium. Although the final pH of the unmodified medium is reduced by 3.4 units, no corrosion was observed on the reactor walls.

Declaration of Competing Interest

The authors declare that they have no known competing financial interests or personal relationships that could have appeared to influence the work reported in this paper.

Data availability

Data will be made available on request.

Acknowledgements

Appendix A. Supporting information

Supplementary data associated with this article can be found in the online version at doi:10.1016/j.supflu.2023.105938.

References

[1] R. Goseki, T. Ishizone, "Poly(methyl methacrylate) (PMMA),". Encyclopedia of Polymeric Nanomaterials, Heidelberg: Springer Berlin Heidelberg,, Berlin, 2014, pp. 1–11, https://doi.org/10.1007/978-3-642-36199-9_244-1.
[2] M.S. Chisdholm, Artificial glass—the versatility of poly(methyl methacrylate) from its early exploitation to the new millennium, J. Chem. Educ. vol. 77 (7) (2000) 841–845, https://doi.org/10.1021/ed077p841.
[3] S. Mattia, A. Sibel, Poly(methyl methacrylate): Market trends and recycling, Adv. Chem. Eng. (2022), https://doi.org/10.1016/bs.ache.2022.09.004.
[4] J. de Tommaso, J.L. Dubois, Risk analysis on PMMA recycling economics, Polymers vol. 13 (16) (2021), https://doi.org/10.3390/polym13162724.
[5] O.P. Korobeinichev, et al., Kinetics of thermal decomposition of PMMA at different heating rates and in a wide temperature range, Thermochim. Acta vol. 671 (2019) 17–25, https://doi.org/10.1016/j.tca.2018.10.019.
[6] U. Ali, K.J.B.A. Karim, N.A. Buang, A review of the properties and applications of poly (Methyl Methacrylate) (PMMA), in: Polymer Reviews., vol. 55, Bellwether Publishing, Ltd,, 02, 2015, pp. 678–705, https://doi.org/10.1080/15583724.2015.1031377.
[7] M.J. Darabi Mahboub, J.L. Dubois, F. Cavani, M. Rostamizadeh, G.S. Patience, Catalysis for the synthesis of methacrylic acid and methyl methacrylate, in: Chemical Society Reviews, vol. 47, Royal Society of Chemistry,, 21, 2018, pp. 7703–7738, https://doi.org/10.1039/c8cs00117k.
[8] E.K.C. Moens, et al., Progress in reaction mechanisms and reactor technologies for thermochemical recycling of poly(methyl methacrylate (MDPI AG), Polymers vol. 12 (8) (01, 2020), https://doi.org/10.3390/POLYM12081667.
[9] M. Kumar, S. Arun, P. Upadhyaya, G. Pugazhenthi, Properties of PMMA/clay nanocomposites prepared using various compatibilizers, Int. J. Mech. Mater. Eng. vol. 10 (no) (2015) 1, https://doi.org/10.1186/s40712-015-0035-x.
[10] L.E. Manring, Thermal degradation of poly(methyl methacrylate). 2. Vinyl-terminated polymer, Macromolecules vol. 22 (6) (1989) 2673–2677, https://doi.org/10.1021/ma00196a024.
[11] T. Kashiwagi, A. Inabi, A. Hamins, Behavior of primary radicals during thermal degradation of poly(methyl methacrylate, Polym. Degrad. Stab. vol. 26 (2) (1989) 161–184, https://doi.org/10.1016/0141-3910(89)90007-4.
[12] E. v Thompson, Dependence of the glass transition temperature of poly(methyl methacrylate) on tacticity and molecular weight, J. Polym. Sci. Part A-2: Polym. Phys. vol. 4 (2) (1966) 199–208, https://doi.org/10.1002/pol.1966.160040204.
[13] S.L. Malhotra, L. Minh, L.P. Blanchard, Thermal decomposition and glass transition temperature of poly(methyl methacrylate) and poly(isobutyl methacrylate),

J. Macromol. Sci.: Part A - Chem. vol. 19 (4) (1983) 579–600, https://doi.org/10.1080/10601328308056536.

[14] X. Lu, B. Jiang, Glass transition temperature and molecular parameters of polymer, Polymer vol. 32 (3) (1991) 471–478, https://doi.org/10.1016/0032-3861(91)90451-N.

[15] G.D. Azevedo, J.C. Pinto, Alkaline hydrolysis of P(VAc-co-MMA) particles for vascular embolization procedures, J. Appl. Polym. Sci. vol. 137 (42) (2020), https://doi.org/10.1002/app.49298.

[16] L. Wadsö, O.J. Karlsson, Alkaline hydrolysis of polymers with ester groups studied by isothermal calorimetry, Polym. Degrad. Stab. vol. 98 (1) (2013) 73–78, https://doi.org/10.1016/j.polymdegradstab.2012.10.031.

[17] S. Pletincx, et al., Unravelling the chemical influence of water on the PMMA/Aluminum oxide hybrid interface in situ, Sci. Rep. vol. 7 (no) (2017) 1, https://doi.org/10.1038/s41598-017-13549-z.

[18] A. Bettencourt, et al., Surface studies on acrylic bone cement, Int J. Pharm. vol. 278 (1) (2004) 181–186, https://doi.org/10.1016/j.ijpharm.2004.03.011.

[19] L.S.A. Smith, V. Schmitz, The effect of water on the glass transition temperature of poly(methyl methacrylate, Polymer vol. 29 (no) (1988) 10, https://doi.org/10.1016/0032-3861(88)90405-3.

[20] J.M. de León, V. Bernardo, E. Laguna-Gutiérrez, M.Á. Rodríguez-Pérez, Influence of the viscosity of poly(methyl methacrylate) on the cellular structure of nanocellular materials, Polym. Int vol. 69 (1) (2020) 72–83, https://doi.org/10.1002/pi.5920.

[21] W.S. Sheu, Molecular weight averages and polydispersity of polymers (Ap), J. Chem. Educ. vol. 78 (4) (2001) 554–555, https://doi.org/10.1021/ed078p554 (Ap).

[22] S.S. Rane, P. Choi, Polydispersity index: How accurately does it measure the breadth of the molecular weight distribution? Chem. Mater. vol. 17 (4) (2005) 926, https://doi.org/10.1021/cm048594i.

[23] J.H. Sim, et al., 1D hypo-crystals: a novel concept for the crystallization of stereo-irregular polymers, Mater. Today vol. 40 (2020) 26–37, https://doi.org/10.1016/j.mattod.2020.05.003.

[24] S. Yousef, J. Eimontas, N. Striügas, S.P. Subadra, M.A. Abdelnaby, Thermal degradation and pyrolysis kinetic behaviour of glass fibre-reinforced thermoplastic resin by TG-FTIR, Py-GC/MS, linear and nonlinear isoconversional models,

[25] N. Katsikis, F. Zahradnik, A. Helmschrott, H. Münstedt, A. Vital, Thermal stability of poly(methyl methacrylate)/silica nano- and microcomposites as investigated by dynamic-mechanical experiments, Polym. Degrad. Stab. vol. 92 (11) (2007) 1966–1976, https://doi.org/10.1016/j.polymdegradstab.2007.08.009.

[26] J.W. Kim, J.Y. Ko, J.B. Jun, I.S. Chang, H.H. Kang, K. do Suh, Multihollow polymer microcapsules by water-in-oil-water emulsions polymerization: Morphological study and entrapment characteristics, Colloid Polym. Sci. vol. 281 (2) (2003) 157–163, https://doi.org/10.1007/s00396-002-0763-3.

[27] J. Biroš, T. Larina, J. Trekoval, J. Pouchly, Colloid & Polymer Science Dependence of the glass transition temperature of poly (methyl methacrylates) on their tacticlty), Colloid Polym. Sci. vol. 260 (1982) 27–30, https://doi.org/10.1007/BF01447672.

[28] Y. Fujii, T. Tominaga, D. Murakami, M. Tanaka, H. Seto, Local dynamics of the hydration water and poly(methyl methacrylate) chains in PMMA networks, Front Chem. vol. 9 (2021), https://doi.org/10.3389/fchem.2021.728738.

[29] D. Ronca, et al., Effect of water uptake on the viscoelastic properties of self-cured PMMA, J. Appl. Biomater. Funct. Mater. vol. 4 (3) (2006) 205–206, https://doi.org/10.1177/228080000600400322.

[30] K. Wondraczek, J. Adams, J. Fuhrmann, Effect of thermal degradation on glass transition temperature of PMMA, Macromol. Chem. Phys. vol. 205 (14) (2004) 1858–1862, https://doi.org/10.1002/macp.200400108.

[31] C. Wang, J.X. Pek, H.M. Chen, W.M. Huang, On-demand tailoring between brittle and ductile of poly(methyl methacrylate) (PMMA) via high temperature stretching, Polymers vol. 14 (5) (2022), https://doi.org/10.3390/polym14050985.

[32] V.N. Novikov, E.A. Rössler, Correlation between glass transition temperature and molecular mass in non-polymeric and polymer glass formers, Polymers vol. 54 (26) (2013) 6987–6991, https://doi.org/10.1016/j.polymer.2013.11.002.

[33] T. Suresh Kumar, M.K. Dash, A. Nagesha, Deformation and damage assessment in type 316 LN stainless steel weld joint under isothermal and thermomechanical cyclic loading, Mater. Sci. Eng. A vol. 849 (2022), https://doi.org/10.1016/j.msea.2022.143494.